DOI: 10.1002/cbic.200900215

Improvement of *Yarrowia lipolytica* Lipase Enantioselectivity by Using Mutagenesis Targeted to the Substrate Binding Site

F. Bordes,[a] E. Cambon,[a] V. Dossat-Létisse,[a] I. André,[a] C. Croux,[a] J. M. Nicaud,[b] and A. Marty*[a]

Lip2p lipase from *Yarrowia lipolytica* was shown to be an efficient catalyst for the resolution of 2-bromo-arylacetic acid esters, an important class of chemical intermediates in the pharmaceutical industry. Enantioselectivity of this lipase was improved by site-directed mutagenesis targeted to the substrate binding site. To guide mutagenesis experiments, the three-dimensional model of this lipase was built by homology modelling techniques by using the structures of lipases from *Rhizomucor miehei* and *Thermomyces lanuginosa* as templates. On the basis of this structural model, five amino acid residues (T88, V94, D97, V232, V285) that form the hydrophobic substrate binding site of the lipase were selected for site-directed mutagenesis. Position 232 was identified as crucial for the discrimination between enantiomers. Variant V232A displayed an enantioselectivity enhanced by one order of magnitude, whereas variant V232L exhibited a selectivity inversion. To further explore the diversity, position 232 was systematically replaced by the 19 possible amino acids. Screening of this library led to the identification of the V232S variant, which has a tremendously increased *E* value compared to the parental enzyme for the resolution of 2-bromo-phenylacetic acid ethyl ester (58-fold) and 2-bromo-*o*-tolylacetic acid ethyl ester (16-fold). In addition to the gain in enantioselectivity, a remarkable increase in velocity was observed (eightfold increase) for both substrates.

Introduction

The need for enantiomerically pure compounds in the pharmaceutical industry has grown since legislation has become more stringent regarding the pharmacological effects of each enantiomer. The market of drugs sold as a single enantiomer represented close to $225 billion worldwide in 2005.[1] The need for new stereoselective enzymes is thus of great interest. Enantiopure carboxylic acid esters are important building blocks for the synthesis of many pharmaceuticals (for instance nonsteroidal anti-inflammatory drugs such as Ibuprofen), pesticides, and natural compounds such as pheromones.[2–5] 2-halogeno-carboxylic acid esters are important intermediates found in the synthetic pathways of a number of drugs such as prostaglandin, prostacyclin, semisynthetic penicillin, and thiazolium salts.[6–9] In particular, 2-bromo-*o*-tolylacetic acid ethyl ester is used as a precursor for the synthesis of analgesics and nonpeptide angiotensin II-receptor antagonists.[10,11]

Recently, we demonstrated that Lip2p lipase from *Yarrowia lipolytica* yeast was an efficient stereoselective enzyme for the resolution of 2-halogeno-arylacetic acid esters.[12] During transesterification of 2-bromo-phenyl-acetic acid ethyl ester with 1-octanol in *n*-octane, an enantioselectivity value (*E* value) of 50 toward the *S*-enantiomer was achieved. Similarly, Lip2p was also able to resolve the racemic mixture of 2-bromo-*o*-tolylacetic acid ethyl ester with an *E* value of 27. It is noteworthy that no commercial lipase was found to be efficient for the resolution of this compound. The best results were obtained with the free lipase from *Burkholderia cepacia*, which led to a poor *E* value (4.3).[11] Of note, activity obtained with *Y. lipolytica* lipase is one order of magnitude higher than that observed with *B. cepacia* lipase.[12] Even if enantioselectivity values obtained with the lipase from *Y. lipolytica* are considered to be promising, they might not be sufficient for an industrial application in the pharmaceutical industry, in which higher purities are required. However, Lip2p could be a good candidate to develop enantioselective catalysts through site-directed mutagenesis or directed evolution. A few directed evolution reports have demonstrated that distant mutations can increase enantioselectivity.[13] Even if no structural knowledge of the enzyme is required beforehand in this approach, the limiting step is, after the creation of a protein library, the screening of thousands of clones to find one enzyme with improved enantioselectivity. Therefore, the easiest and usually the most efficient way to improve the discrimination between enantiomers con-

[a] *Dr. F. Bordes,[+] Dr. E. Cambon,[+] Dr. V. Dossat-Létisse, Dr. I. André, Dr. C. Croux, Prof. A. Marty*
Université de Toulouse; INSA, UPS, INP; LISBP
135 Avenue de Rangueil, 31077 Toulouse (France)
INRA, UMR792 Ingénierie des Systèmes Biologiques et des Procédés.
CNRS, UMR5504
31400 Toulouse (France)
Fax: (+33) 5-61-55-94-00
E-mail: alain.marty@insa-toulouse.fr

[b] *Dr. J. M. Nicaud*
Laboratoire de Microbiologie et Génétique Moléculaire
CNRS-INRA-INAPG UMR 2585
78850 Thieverval-Grignon (France)

[+] *These authors contributed equally to this work.*

sists in the modification by site-directed mutagenesis of amino acids located directly in the active site.[14–16]

The strategy followed in the present study aims at applying site-directed mutagenesis to amino acid residues located at the substrate binding site to obtain variants of Lip2p lipase with improved enantiopreference for the resolution of 2-bromo arylacetic acid ethyl ester and compatible with an industrial application in the pharmaceutical industry. Given the absence of crystallographic data on Lip2p lipase, a three-dimensional model was built by using homology modelling with the X-ray structures of highly similar lipases as templates. On the basis of a structural analysis of Lip2p model in complex with substrates of interest, amino acid residues from the active site were selected and modified to create Lip2p variants which were subsequently evaluated for the resolution of the 2-bromo arylacetic acid ethyl ester derivatives.

Results and Discussion

Homology modelling of Lip2p from *Y. lipolytica*

The crucial starting point of a homology modelling strategy is the identification of related proteins in the Protein DataBank (PDB) that could be selected as templates. The Lip2p sequence was submitted for a search against the Protein DataBank using the PSI-BLAST algorithm.[17] As a result, three lipases of known 3D-structure and one feruloyl esterase were identified as having a significant homology with Lip2p and were thus selected as templates for homology modelling of Lip2p. All three identified lipases belong to the fungal lipase family: lipases from *Rhizomucor miehei* (*Rm*LIP, PDB codes: 3TGL and 4TGL; sequence identity 29%, sequence homology 46%, gap 16%), *Rhizopus niveus* (*Rn*LIP, PDB ID: 1LGY; sequence identity 33%, sequence homology 47%, gap 17%) and *Thermomyces lanuginosa* (*Tl*LIP, PDB ID: 1GT6), (sequence identity 31%, sequence homology 47%, gap 14%). The feruloyl esterase from *Aspergillus niger* (PDB ID: 1USW) also revealed a similarity with Lip2p lipase (sequence identity 30%, sequence homology 46%, gap 10%).

The multiple sequence alignment of proteins identified by the PSI-BLAST search against the Lip2p sequence is shown in Figure 1.

The secondary structure pattern appears to be very well conserved amongst all five enzymes. This multiple alignment allowed the identification of five catalytically important amino acid residues that form the conserved catalytic triad and the oxyanion hole. The catalytic Ser of Lip2p, located in the nucleophilic elbow after β-strand 5, was easily identified as Ser162 by the well-known GxSxG lipase signature. In the case of Lip2p, this signature is GHSLG, like for other lipases from the filamentous fungi superfamily. The two other amino acids of the catalytic triad are perfectly aligned with the catalytic residues of other proteins, namely Asp230 and His289 located after β-strands 7 and 8, respectively. Another important region of lipases is the oxyanion hole, which consists in two residues that give their backbone amide protons to stabilize the tetrahedral intermediate formed during the reaction mechanism. One of these residues is positioned identically in all lipases, next to the catalytic Ser. Like in mucoral lipases, this residue is a Leu (Leu163) in Lip2p. The second residue of the oxyanion hole is located in a loop after the β-strand 3, and next to a Gly residue. As for filamentous fungi, this second residue which forms the oxyanion hole in Lip2p is a rather hydrophilic residue, Thr88, corresponding to Ser82, Ser83 and Thr82 in *R. miehei*, *T. lanuginosa* and *R. niveus* lipases, respectively.

Like other mucoral lipases, Lip2p belongs to the "GX" type lipase, which bears specificities for medium and long chains.[18] Indeed, *Y. lipolytica* lipase presents a tenfold higher activity for triolein than for tributyrin.[12] In contrast, Lip1p from *Y. lipolytica* belongs to the GGGX type which displays specificities for short chains according to the classification proposed by Pleiss et al.[18] In the open form of mucoral lipases, the side chain of the hydrophilic residue of the oxyanion hole interacts through a hydrogen bonding interaction with a hydrophilic residue, called the anchor residue, which is located at the end of the α-helix B′1 and forms the lid of the lipase (Asp91 in *R. miehei* and *R. niveus* lipases and Asn92 in *T. lanuginosa* lipase). In Lip2p from *Y. lipolytica* this so-called anchor residue could be played by Asp97 as suggested by sequence alignment (Figure 1).

Lip2p from *Y. lipolytica* is an excreted protein. These proteins are known to generally contain numerous disulfide bonds in eukaryotes. Disulfide bonds play an essential structural role within proteins by stabilizing their tertiary structure, and the correct disulfide bridge organization is thus crucial to maintain protein structure and function. Altogether, *Y. lipolytica* lipase contains nine Cys residues. Structural alignment of Lip2p from *Y. lipolytica* with other homologous lipases revealed that disulfide bridges corresponding to Cys30–Cys299 and Cys43–Cys47 in *Y. lipolytica* lipase are found in all homologous lipases. The Cys265–Cys273 disulfide bridge is only found in *R. miehei* and *R. niveus* lipases while the Cys120–Cys123 disulfide bridge is only observed in *T. lanuginosa* lipase (Figure 2). Cys244 appears to be the only free Cys of Lip2p. Therefore, it can be assumed from this alignment that Lip2p lipase from *Y. lipolytica* is stabilized by four disulfide bonds (Cys30–Cys299, Cys43–Cys47, Cys120–Cys123, Cys265–Cys273), and contains one free Cys (Cys244). Such formation of disulfide bonds is a key step in protein folding, and an insight on the organization of the disulfide bonds is crucial for the building by homology modelling of the enzyme 3D model. The presence of these four disulfide bonds was thus postulated in order to build the 3D structure of the active Lip2p protein.

In most lipases, a mobile element consisting in one or two short helices covers the catalytic active site. This lid that blocks the active site in the closed form of the enzyme has been shown to move away in presence of a hydrophobic interface, to adopt an open conformation where the active site becomes accessible to the substrate. All three filamentous fungi lipases identified by the PSI-BLAST search contain this so-called lid, identified as Ile86–Leu93 in *T. lanuginosa* lipase, Ile85–Asp91 in *R. meihei* lipase and Phe85–Asp91 in *R. niveus* lipases On the basis of the alignment, the α-helix formed by residues comprised between Leu91 and Asp97 was assumed to play the role of the lid in *Y. lipolytica* lipase.


```
Y.l.:   1  VYTSTETSHIDQESY-NFFEKYARLANIGY---C--VGPGTKIFKPFNC-GLQCAH--FPNVELIEEFHDPRLIF  66
T.l.:   3            SQDLFNQFNLFAQYSAAAY---CGKNNDAPAG-TNITCTGNACPEVEKADATFLYSFED-SGVG  61
R.m.:   1   SINGGIRAATSQEI-NELTYYTTLSANSY---CRTVIPGAT----WDC--IHCDA--TEDLKIIKTWST--LIY  60
R.n.:   1   SDGGKVVAATTAQI-QEFTKYAGIAATAY---CRSVVPGNK----WDC--VQCQKWVPDGKIITTFTS---LLS  61
USW             ASTQGISEDLYNRLVEMATISQAAYADLCNIPST--------IIKGEKIYNAQT-------------     46

Y.l.:  67  DVSGYLAVDHASKQIYLVIRGTHSLEDVITDIRIMQAPLTN--FDLAANISSTATCDDCLVHNGFIQSYNNTYN 138
T.l.:  62  DVTGFLALDNTNKLIVLSFRGSRSIENWIGNLNFDLKEIND-------------ICSGCRGHDGFTSSWRSVAD 122
R.m.:  61  DTNAMVARGDSEKTIYIVFRGSSSIRNWIADLTFVPVSYPP-------------VSGTKVHKGFLDSYGEVQN 120
R.n.:  62  DTNGYVLRSDKQKTIYLVFRGTNSFRSAITDIVFNFSDYKP-------------VKGAKVHAGFLSSYEQVVN 121
USW        DINGWILRDDTSKEIITVFRGTGSDTNLQLDTNYTLTPFDT-----------LPQCNDCEVHGGYYIGWISVQD
1put                 SKVVYVSHDGTRRQLDVADGVSLMQAAVSNGIYDIVGDCGGSASCATCHVY

Y.l.: 139  QIGPKLDSVIEQYPDYQIAVTGHSLGGAAALLFGINLK-----VNGHDPLVVTLGQPIVG 193
T.l.: 123  TLRQKVEDAVREHPDYRVVFTGHSLGGALATVAGADLR-----GNGYDIDVFSYYAPRVG 177
R.m.: 121  ELVATVLDQFKQYPSYKVAVTGHSLGGATALLCALDLYQREEGLSSSNLFLYTQGQPRVG 180
R.n.: 122  DYFPVVQEQLTAHPTYKVIVTGHSLGGAQALLAGMDLYQREPRLSPKNLSIFTVGGPRVG 181
USW        QVESLVKQQASQYPDYALTVTGHSLGASMAALTAAQLS--ATYD---NVRLYTFGEPRSG

Y.l.: 194  NAGFANWVDKLFFGQENPDVSKVSKDRKLYRITHRGDIVPQV-PFWDGYQHCSGEVFIDWPLIHPP-LSNVVMCQ 266
T.l.: 178  NRAFAEFLTV-------------QTGGTLYRITHTNDIVPRLPPREFGYSHSSPEYWIKSGTLVPVTRNDIVKIE 239
R.m.: 181  NPAFANYVVST-------------GIPYRRTVNERDIVPHLPPAAFGFLHAGSEYWITDN---SP--ETVQVCT 236
R.n.: 182  NPTFAYYVEST-------------GIPFQRTVHKRDIVPHVPPQSFGFLHPGVESWI---KSGTS---NVQICT 236
USW        NQAFASYMNDAFQVSS-------PETTQYFRVTHSNDGIPNLPPADEGYAHGGVEYWSVD----PYSAQNTFVCT

Y.l.: 267  GQ-SNKQCSAGNTLLQQVNVIGNHLQYF-VTEGVC 299
T.l.: 240  GI-DATGGNNQPNI---PDIP-AHLWYFGL-IGTC 268
R.m.: 237  SDLETSDCS--NSIVPFTSVL-DHLSYFGINTGLC 268
R.n.: 237  SEIETKDCS--NSIVPFTSIL-DHLSYFDINEGSC 268
USW        GD- EVQCCEAQGGQ--GVND-AHTTYFGMTSGACTW
```

Figure 1. Multiple sequence alignment of lipases from *Yarrowia lipolytica* (*Y.l.*), *Thermomyces lanuginosa* (*T.l.*), *Rhizomucor miehei* (*R.m.*), *Rhizopus niveus* (*R.n.*), the feruloyl esterase from *Aspergillus niger* (1USW) and a fragment from a putidaredoxin from *Pseudomonas putida* (1PUT). Residues forming part of α-helices and β-strands are coloured in magenta and green, respectively. The three catalytic residues are coloured in red, the two catalytic residue of the oxyanion hole in orange, the cysteines are blue-coloured and the lid is underlined.

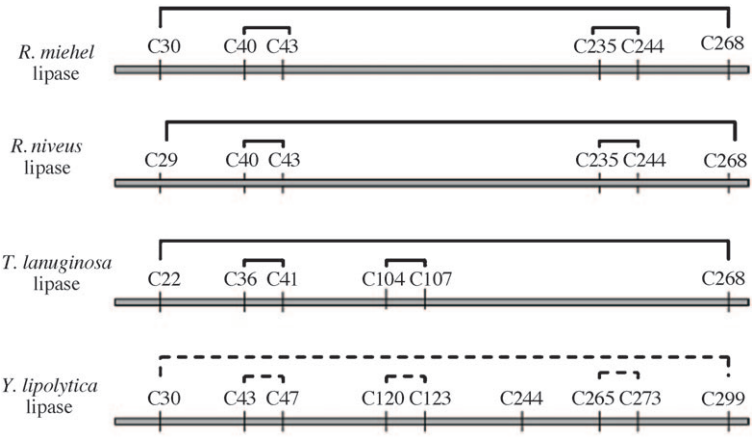

Figure 2. Disulfide bond alignments of lipases from the fungal family.

Our interest was to obtain a model of the open form of *Y. lipolytica* lipase in order to shed some light on the molecular determinants involved in enantiomer discrimination. Only *R. miehei* (4TGL) and *T. lanuginosa* (1GT6) lipases were co-crystallized in their open forms with diethylphosphonate inhibitor and oleic acid, respectively, in their active sites. By using the crystallographic coordinates of these lipases, the three-dimensional model of Lip2p lipase from *Y. lipolytica* was constructed. A fragment from the putidaredoxin (1PUT) was also used for the construction of the loop between amino acids 107 and 119. The lowest energy model of Lip2p built using MODELLER was further refined using the CFF91 force field implemented within the DISCOVER module of InsightII suite of programs (Accelrys, San Diego, CA, USA). The predicted model was then checked for main chain conformations using the PROCHECK software implemented in the Biotech Validation Suite for Protein Structures.[19] The geometry analysis showed that initially close to 97% of the Φ–Ψ plots were in the core regions, and less than 3% fell into the generously allowed and disallowed regions of the Ramachandran's plot. Most of the residues which were in the generously allowed and disallowed regions belonged to the loop regions in which major insertions and deletions were made. A further refinement of the main chain conformations was performed selectively in these regions, and Φ–Ψ plots of all the nonglycine residues of the modelled structure which were initially in the disallowed regions were corrected. Side-chain planarity of the planar groups in aromatic rings (Phe, Tyr, Trp, His) and planar end groups (Arg, Asn, Asp, Gln, Glu) were checked using PROCHECK. Deviations from planarity were identified by measuring root mean square (RMS) distances of planar atoms from the best fitted plane. Residues having RMS distances greater than 0.03 Å for rings and 0.02 Å for other groups were

marked as outliers.[19] The modelled structure showed a reasonably acceptable number of outliers compared to X-ray structures of *R. miehei*, *T. lanuginosa*, and *R. niveus* lipases. RMS deviations (RMSD) of bond lengths and bond angles of all modelled structure were within 0.02 Å and 3.5 degrees respectively from the standard values; this indicates reasonably good structural parameters. A rotamer check was performed using WHATIF implemented in the Biotech Validation Suite for Protein Structures.[20] This indicated the presence of only two rotamer outliers in our modelled structure. The overall protein fold of Lip2p is shown in Figure 3.

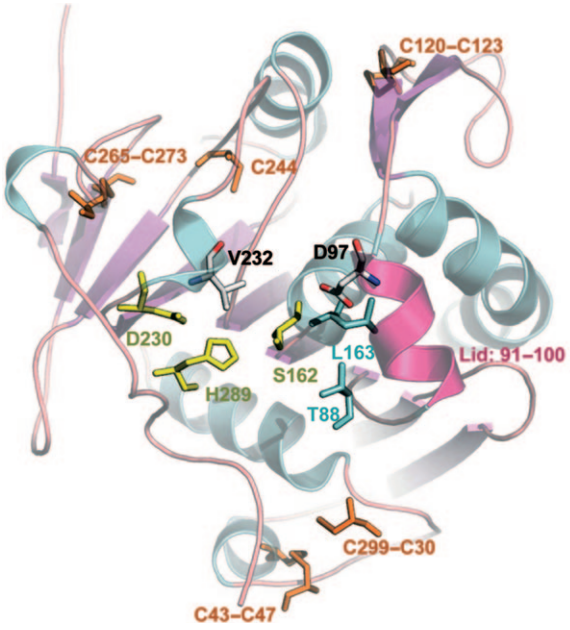

Figure 3. Overall representation of the Lip2p homology model. Hydrogen atoms on amino acid residues have been omitted for clarity purpose.

The substrate binding site appears as a hydrophobic crevice located at the protein surface, with a catalytic triad exposed to the solvent, like in mucoral lipases such as *R. miehei* lipase. The hydrophobic crevice consists of T88, V94, I98, I100, F129, L163, P190, V232, V235, P236, Y241 corresponding to S82, W88, L92, F94, F111, L145, P177, V205, L208, P209 and F215 in *R. miehei* lipase.[21] The scissile fatty acid of a triglyceride is supposed to bind to this hydrophobic crevice. The *sn*-2 substituent would bind to the hydrophobic dent formed by I204, T252, V254 and L258 in *R. miehei* lipase and by I231, V283, V285 and L290.[21] Figure 4 represents the superimposition of Lip2p and lipases from *Rhizomucor miehei* and *Thermomyces lanuginosa* lipases.

The overall structures are similar, the core of the fold is largely conserved and as expected, the most significant differences are seen in the regions of the surface loops. The three catalytic residues and the two amino acids involved in the oxyanion hole are perfectly superposed.

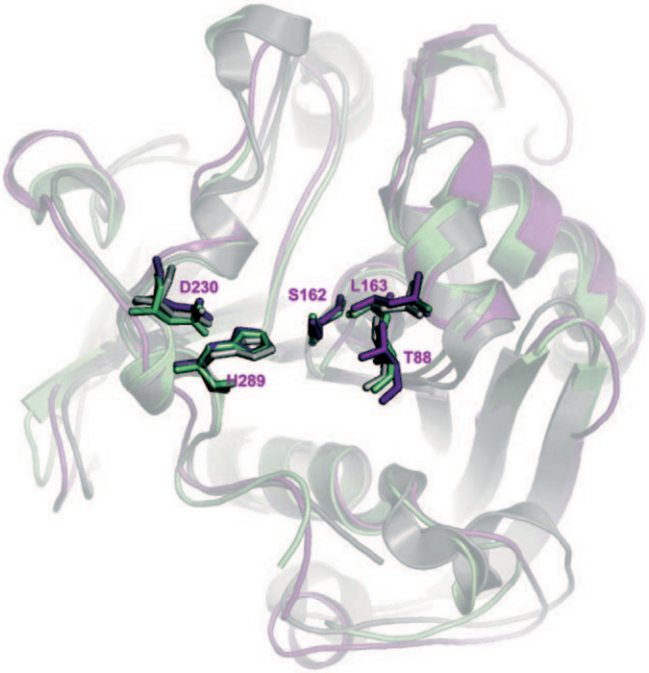

Figure 4. Superimposition of Lip2p (colored in magenta) and lipases from *Rhizomucor miehei* (colored in green) and *Thermomyces lanuginosa* (colored in gray). Catalytic residues and amino acids involved in oxyanion stabilization are superposed. Hydrogen atoms on amino acid residues have been omitted for clarity purpose.

Improvement of Lip2p enantioselectivity

Site-directed mutagenesis targeted at the substrate binding site: The covalent intermediates between the Lip2p catalytic Ser (Ser162) and the (*R,S*)-2-bromo-phenylacetic acid ethyl esters were constructed and refined using a standard energy minimization procedure. The five hydrogen bonding interactions described as being crucial for the stabilization of the tetrahedral intermediate are observed for both the *R*- and the *S*- substrates (Figure 5). The alcohol group of the ester function and the phenyl group are oriented towards the exterior of the active site. A detailed analysis of the resulting complexes was used to guide the selection of the most promising amino acid residues of Lip2p to be targeted by site-directed mutagenesis. On the basis of our analysis, we have focused our attention on residues located in the active site and in direct contact with the substrate. Altogether five amino acid residues (Thr88, Val94, Asp97, Val232 and Val285) potentially involved in enzyme–substrate interactions that could likely play a role on enzyme selectivity were identified (Figure 5). The three Val residues (Val94, Val232 and Val285) were independently changed into Ala and Leu residues, while Thr88, the first residue of the oxyanion hole, was replaced by Ser, Leu, Val or Ala and Asp97 was replaced by Ala. The objective of such amino acid replacements was to open up or to further restrain the active site topology in order to alter the enantiopreference.

Variant activities were measured using the classical test of *p*-nitrophenol (*p*NP) butyrate hydrolysis (Table 1). Replacement of the putative second residue of the oxyanion hole Thr88 by Ala, Val or Leu residues led to a complete loss of Lip2p activity.

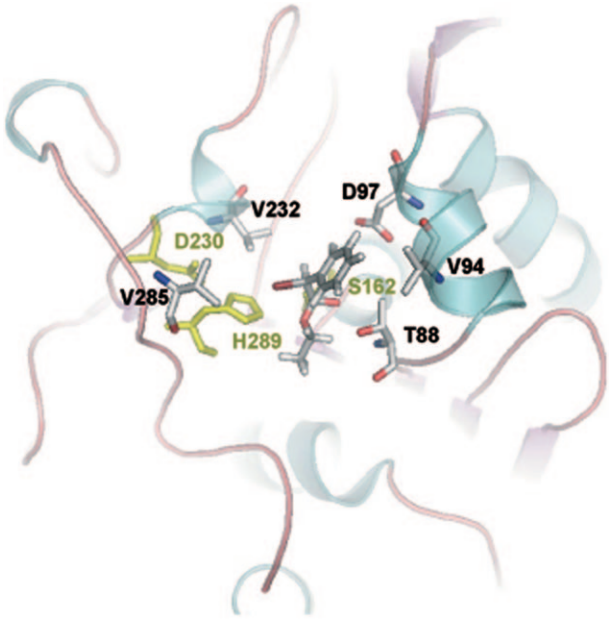

Figure 5. Representation of Lip2p amino acid residues selected for site-directed mutagenesis. The *S*-2-bromo-phenylacetic acid ethyl ester covalently bound to Ser162 is shown in the active site.

However, substitution of this residue by a Ser enabled one third of the activity to be maintained. These results clearly demonstrate that the presence of a hydrophilic residue at this key catalytic position, such as Ser or a Thr, is crucial for activity even though the residue side chain does not interact directly with the substrate. These results are in agreement with prior reports on lipases from filamentous fungi.[22–23] Similarly, the exchange of Thr by Ser in *R. delemar* lipase led to a low decrease in activity, while the replacement by a hydrophobic residue resulted in a loss of activity.[22–23] In an earlier report, Pleiss et al.[18] suggested that in this lipase superfamily, the hydrophilic oxyanion hole residue (Ser or Thr) is within hydrogen bonding distance from the hydrophilic anchor residue (Asp or Asn); thus, this leads to the stabilization of the oxyanion hole. In our model of Lip2p, such hydrogen bonding interaction has not been observed. The variant T88S displayed higher activities for the resolution of both racemic mixtures of 2-bromo-phenyl and *o*-tolyl acetic acid ethyl esters (Tables 2 and 3). However, enantioselectivity values were decreased for both substrates.

Changes at positions 94 and 285 showed no significant influence on *p*NP butyrate hydrolysis (Table 1) nor on activity and enantioselectivity during racemic mixture resolution (Tables 2 and 3). Changes of these amino acids positioned at the entrance of the active site by similarly hydrophobic amino acids did not affect enzyme activity and selectivity.

Table 1. *p*-Nitrophenol butyrate hydrolysis activity of wild-type Lip2p and its variants.

Enzyme	WT	T88S	T88X[c]	V94A	V94L	V285A	V285L	V232A	V232L	D97A
Initial rate[a,b]	64.0	21.3	0	52.8	42.5	46.0	45.6	47.4	40.3	9.8

[a] μmol of *p*NP liberated per minute and mL of enzyme. [b] Each experiment was carried out in triplicate. [c] X = A, V, L.

Table 2. 2-bromo-phenylacetic acid ethyl ester hydrolysis activity of wild-type Lip2p and its variants.

Enzyme	WT	T88S	V94A	V94L	V285A	V285L	V232A	V232L	D97A
vi*S*[a]	1.71	2.13	1.41	1	0.97	1.3	8.8	0.017	0.010
vi*R*[a]	0.58	1.04	0.39	0.44	0.4	0.4	0.101	0.31	0.34
E value[b]	3(*S*)	2(*S*)	4(*S*)	2(*S*)	2(*S*)	3(*S*)	87(*S*)	18(*R*)	34(*R*)
conversion [%]	54.7 (8 h)						52.9 (8.5 h)		
ee_s[c] [%]	53.5						99.6		
ee_p[d] [%]	43.7						88.7		

[a] μmol of 2-bromo-phenylacetic acid liberated per hour and mL of enzyme. [b] *E* value = vi*S*/vi*R* or vi*R*/vi*S* according to enantiomer preference; vi*R*, vi*S*: initial rates. [c] Substrate enantiomeric excess. [d] Product enantiomeric excess.

Table 3. 2-bromo-*o*-tolylacetic acid ethyl ester hydrolysis activity of wild-type Lip2p and its variants.

Enzyme	WT	T88S	V94A	V94L	V285A	V285L	V232A	V232L	D97A
vi*S*[a]	0.105	0.167	0.099	0.051	0.12	0.072	1.38	0.001	0.002
vi*R*[a]	0.007	0.04	0.007	0.007	0.007	0.005	0.015	0.001	0.04
E value[b]	16(*S*)	4(*S*)	15(*S*)	8(*S*)	16(*S*)	16(*S*)	92(*S*)	1	20(*R*)
conversion [%]							53.5 (24 h)		
ee_s[c] [%]							98.6		
ee_p[d] [%]							87.7		

[a] μmol of 2-bromo-*O*-tolylacetic acid liberated per hour and mL of enzyme. [b] [E value = Vi*S*/Vi*R* or Vi*R*/Vi*S* according to enantiomer preference; vi*R*, vi*S*: initial rates. [c] Substrate enantiomeric excess. [d] Product enantiomeric excess.

Similarly, replacement of V232 by hydrophobic amino acids such as Ala or Leu did not markedly influence the enzyme activity during *p*NPB hydrolysis. Variants V232A and V232L displayed an activity reduced from respectively 74% and 63% of wild-type Lip2p activity. It is noteworthy that position 97 appeared more sensitive, as variant D97A displayed no more than 11% of the activity of the parental enzyme (Table 1). Even if this variant is still active, these results support the stabilizing role suggested for D97 anchor residue.

Overall, these results reveal the key role of positions 97 and 232 for both the activity and the enantioselectivity of Lip2p during the resolution of the racemic mixture of 2-bromo-phenylacetic acid ethyl ester (Table 2). Indeed, a small change of the parental V232 residue into an Ala enabled a remarkable increase in enantioselectivity by an order of magnitude, going from an *E* value of three for the wild-type enzyme to 87 for the V232A variant. An improvement in enantioselectivity is often accompanied by a decrease in enzyme activity, as improvement in enantioselectivity often comes as the result of an activity loss for the worst enantiomer. However, no such effect has been observed in the case of V232A variant: it displayed a fivefold enhanced activity toward the *S*-enantiomer, whereas its activity toward the *R*-enantiomer is about six times lower than that obtained using the wild-type Lip2p. Enantiomeric excesses of the substrate and the product are 99.6% and 88.7%, respectively, at 52.9% total conversion after 8.5 h of reaction. At this point in time, 94% of *R*-substrate can be recovered with a purity of 99.8%, and 99.8% at 94.3% purity for the *S*-product. Performances of this variant were analysed in more details in a prior report.[24] Influence of the ester group was investigated: replacement of the ethyl group by an octyl group had slight influence on the activity and on the selectivity of the variant, whereas the presence of a benzyl group led to a decrease in both its activity and its selectivity.[24]

Reversely, replacement of V232 by a bulkier amino acid such as Leu led to an inversion of the enantiopreference (*E* value 18), mainly caused by a drastic 100-fold drop in the catalysis of the wild-type enzyme preferred *S*-enantiomer. The variant D97A enabled also enantiopreference to be reversed for this racemic mixture due to a drastic decrease in the catalysis of the *S*-enantiomer (Table 2).

During the resolution of the racemic mixture of 2-bromo-*o*-tolylacetic acid ethyl ester, variant V232A also exhibited higher activity and enantioselectivity. In this case, improvement in enantioselectivity from an *E* value of 16 for the wild-type enzyme to 92 for the V232A variant is exclusively due to a better catalysis of the preferred *S* enantiomer (13 times higher), although catalysis of poorly recognized *R* enantiomer was also found to be increased by twofold. After 24 h, the conversion is 53.5% with enantiomeric excesses of 98.6 and 87.7 for substrate and product, respectively. 93% of the *R* substrate can be recovered with a purity of 99.3%, and 99.3% at 93.8%

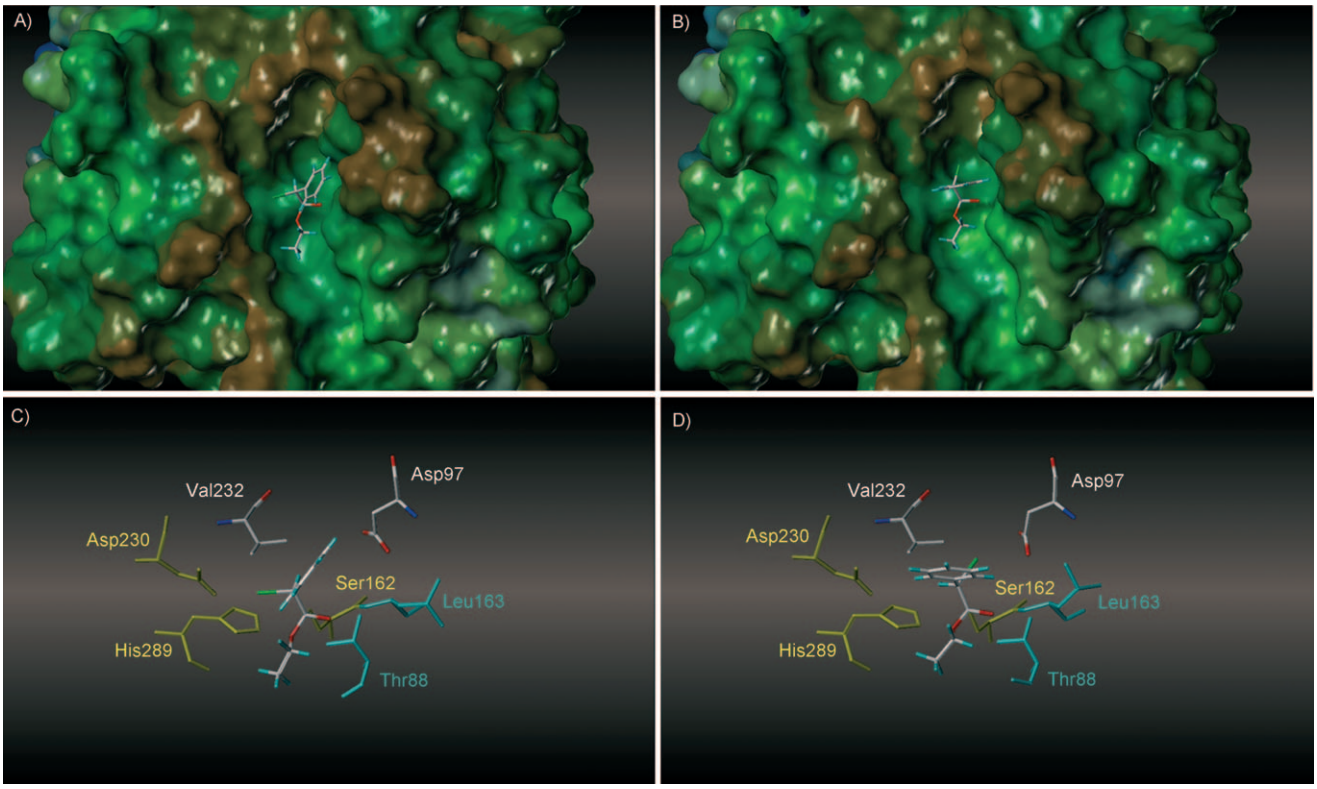

Figure 6. Representation of (*R*,*S*)-2-bromo-phenylacetic acid ethyl ester enantiomers covalently bound to catalytic Ser162 of Lip2p. A), B) *S* and *R* enantiomers are respectively shown. Lip2p is shown as a Connolly surface mapped with the lipophilic potential, as calculated by the MOLCAD module implemented in SybyL7.3 (Tripos, Saint Louis, USA). The protein surface is colour-coded (brown colour indicates more lipophilic regions whereas blue codes for more polar ones). C), D) Arrangement of the *S* (left) and *R* (right) enantiomers with respect to the catalytic triad (coloured in yellow) as well as the residues forming the oxyanion hole (cyan coloured) and the two key positions (V232 and D97) playing a role on enantio-discrimination.

purity for the *S* product. For this racemic mixture the variant V232L showed no activity whereas variant D97A displayed an inversion of the enantiopreference.

In Figure 6 the energy-minimized covalent intermediates of Lip2p with *R* and *S* enantiomers of 2-bromo phenylacetic acid ethyl ester are shown. From these docking modes, the bulky bromine atom positioning appears to be involved in the discrimination between enantiomers. For the *S* enantiomer, the bromine atom is facing Val232 (Figure 6 A and C). The size of this amino acid appears to be crucial for the positioning of the *S*-enantiomer; the discrimination mechanism is a very sensitive system. A smaller amino acid, like Ala, improves the positioning of the *S* enantiomer in the active site, which leads to an increase in its catalysis. On the contrary, introduction of a Leu at position 232 restrains the enzyme active site, impairing the recognition of the *S* enantiomer by the enzyme. The role played by residue 97 in the discrimination of enantiomers is not clearly apparent (Figure 6 B and D). Indeed, the enantioselectivity reversion is mainly due to the poor catalysis of the *S* enantiomer, which cannot easily be explained by the 3D model.

Systematic exploration of position 232: In the first part of this work, one key position (V232) was identified for the discrimination of two racemates of pharmaceutical interest, namely 2-bromo phenyl and *o*-tolyl acid esters. To gain a deeper insight on the role played by this amino acid in Lip2p enantioselectivity, a replacement of V232 by the other 19 possible amino acids was investigated. Saturation mutagenesis techniques were discarded. Indeed even if an optimal use of degenerated codons permits to reduce greatly the number of clones to screen,[25] this process is still time consuming and require the development of high throughput screening procedures. The systematic replacement of V232 by other 19 possible amino acids was undertaken using site directed mutagenesis. A library of 19 monomutants was built and expressed in the recently developed *Y. lipolytica* strain JMY1212.[26] The use of this strain enables the expression cassette containing the lipase gene to be introduced in a single copy at the zeta docking platform at the LEU2 locus in the genome. After transformation, three transformants were randomly chosen and cultivated for lipase expression. The activity coefficient of variance was lower than 5 % (data not shown).

Figures 7 and 8 show the screening results of the V232 monomutant library for the hydrolysis of the 2-bromo- phenylacetic and the 2-bromo-*o*-tolylacetic acid ethyl esters, respectively. Most variants showed a very low activity and selectivity toward both substrates and were thus not detected (variants V232 D, E, K, R, H, Q, W, N, P, M and Y). In addition, variants V232L, I and F that showed lowest hydrolytic activities towards phenylacetic acid ethyl ester did not reveal any hydrolytic activity for the racemic mixture of *o*-tolyl acid ester.

Two variants, V232G and V232S, exhibited a significant enhancement in selectivity compared to the earlier described variant V232A[24] (Figure 7) for the resolution of 2-bromo-phenylacetic ester racemate. Compared to the wild-type Lip2p, an *E* value increase of 32- and 58-fold for variants V232G and V232S, respectively, was achieved for the resolution of the 2-bromo-phenylacetic ester racemate. It is noteworthy that

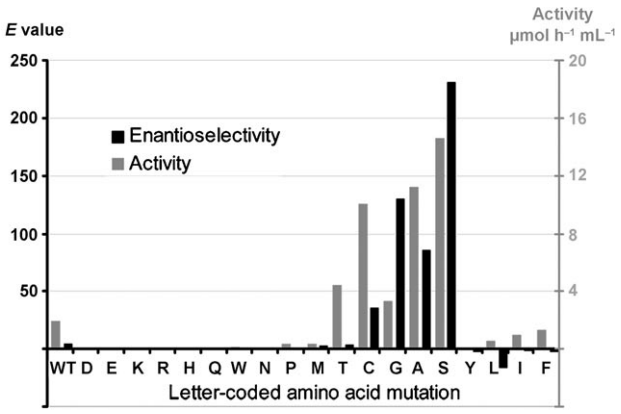

Figure 7. Activity and enantioselectivity of V232 variants in 2-bromo-phenylacetic octyl ester racemate hydrolysis reaction. WT: wild-type Lip2p. A positive *E* value corresponds to *S* selectivity, a negative *E* value to *R* selectivity.

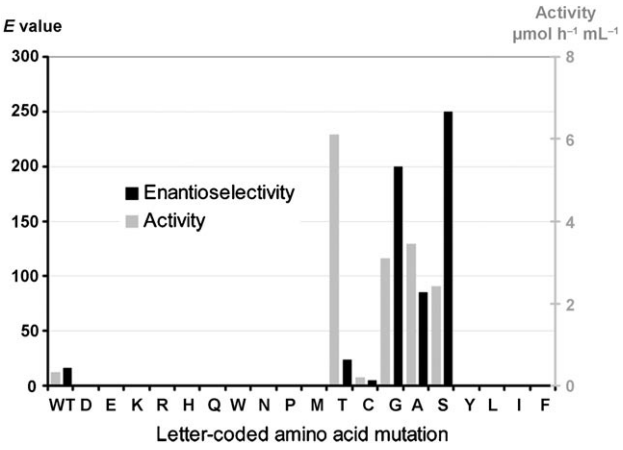

Figure 8. Activity and enantioselectivity of V232 variants in 2-bromo-*o*-tolylacetic octyl ester racemate hydrolysis reaction. WT: wild-type Lip2p. A positive *E* value corresponds to *S* selectivity, a negative *E* value to *R* selectivity.

V232Y, V232L, V232I, V232F variants displayed an inverted selectivity toward the *S*-enantiomer with *E* values of 2.5, 16, 2 and 2.5, respectively.

Regarding the resolution of 2-bromo-*o*-tolylacetic acid ethyl esters racemate, the variant V232S emerges as the best variant with an *E* value of 250, a 16-fold increase in enantioselectivity compared to the wild type enzyme (Figure 8). Interestingly, variant V232T appeared significantly more active than the wild enzyme (with a 19-fold increase in activity) for the catalysis of the *o*-tolyl acid ester but its enantioselectivity was quite low.

This paper describes a successful rational design approach to increase enzyme enantioselectivity guided by homology modeling. One original finding was to be able to increase enantioselectivity one or two orders of magnitude by changing only one amino acid. A second finding is that the improved E value is the consequence of increased reaction rate of the fast-reacting enantiomer with the nice consequence that enantioselectivity improvement is accompanied by a eightfold increase in velocity. Variant V232S is now compatible with industrial application in the pharmaceutical industry.

Overall, these results indicate that the size of the amino acid at position 232 is clearly of importance rather than its polarity. Substitution by small amino acid residues such as a Gly, Ala or Ser enabled a better recognition of the *S* enantiomer; this emphasizes the sterically controlled recognition of the *S*-enantiomer during catalysis. On the other hand, the presence of a bulkier amino acid such as a Leu, Ile or a Phe led to an inversion of enantiopreference. Discrimination between enantiomers is in this case a very accurate process and clearly position 232 is crucial.

Position 97 also appeared to have an influence on enantioselectivity, leading to reversion of enantiopreference. Saturation at this position was also realised but the best variant was the variant D97A earlier described.

We are currently working on the determination of the crystallographic structure of this lipase in order to improve our knowledge on the key structural determinants involved in enantioselectivity at a molecular level.

Experimental Section

Chemical reagents: Yeast extract and tryptone were purchased from Difco (Sparks, USA), oleic acid from Prolabo (Fontenay sous Bois, France), Tween-40 and *n*-octane from Sigma. *n*-Octane was dried over molecular sieves (3 Å) before use.

The procedures for the preparations of (±)-2-bromo phenylacetic acid ethyl and octyl esters as well as (±)-2-bromo-*o*/*m*/*p*-tolylacetic acid ethyl and octyl esters were previously described[11]

Construction of Lip2p variants: The plasmid JMP8 containing the expression cassette carrying the wild-type *LIP2* gene is described elsewhere.[27]The gene *LIP2* encoding the extracellular lipase Lip2p was placed under the transcriptional control of the strong promoter POX2 inducible by oleic acid. The derivative plasmids JMP8V232A, JMP8V232L, JMP8V94A, JMP8V94L, JMP8V285A, JMP8V285L, JMP8-T88A, JMP8-T88S and those relative to saturation mutagenesis at the position 232 carrying single amino acid changes in the *LIP2* gene were constructed by site-directed mutagenesis using the QuikChange™ site-directed mutagenesis kit (Stratagene). The procedure utilized the JMP8 double-stranded DNA vector and two synthetic oligonucleotide primers, each complementary to opposite strands of the vector. Primers contained the desired mutation (underlined in the following sequences). The following primers and their complementary reverse counterparts were used to construct the variant enzymes:

V232A_for: 5′-GGA GAT ATC GCC CCT CAA GTG CCC TTC TGG GAC GGC TAC CAG CAC TGC-3; V232L for: 5′-GGA GAT ATC CTC CCT CAA GTG CCC TTC TGG GAC GGC TAC CAG CAC TGC-3; V94A for: 5′-TCG AGG AAC CCA CTC TCT CGA GGA CGC CAT AAC CGA CAT CCG-3; V94L for: 5′-TCG AGG AAC CCA CTC TCT CGA GGA CCT CAT AAC CGA CAT CCG-3; V285A for: 5′-CTC CAG CAG GTC AAT GCC ATT GGT AAC CAT CTG CAG TAC-3; V285L for: 5′-CTC CAG CAG GTC AAT CTG ATT GGT AAC CAT CTG CAG TAC-3; T88A for: 5′-CCT TGT TAT TCG AGG AGC CCA CTC TCT CGA GGA CGT CAT AAC CG-3; T88S for: 5′-CCT TGT TAT TCG AGG ATC CCA CTC TCT GGA GG-3.

The following primers and their complementary reverse counterpart were used for systematic directed mutagenesis at position 232:

5′-CGA GGA GAT ATC **XXX** CCT CAA GTG CCC-3′ with XXX being GCC for V232A, TGC for V232C, GAC for V232D, GAG for V232E, TTC for V232F, GGC for V232G, CAC for V232H, ATC for V232I, AAG for V232K, CTC for V232L, ATG for V232M, AAC for V232N, CCC for V232P, CAG for V232Q, CGA for V232R, TCC for V232S, ACC for V232T, TGG for V232W, TAC for V232Y.

Mutations were confirmed by DNA sequencing (Genome Express, Grenoble, France).

E. coli DH5α was used as the host to produce the different plasmids. The plasmids were digested with NotI and used for transformation of strain JMY1212 (*MATA ura3–302 leu2–270-LEU2*-zeta *xpr2–322 Δlip2 Δlip7Δ lip8*)[26] by the lithium acetate method as described previously.[8]

Erlenmeyer flasks (500 mL) containing medium $Y_1T_2O_2$ (50 mL total) made of yeast extract (10 g L^{-1}), bactotryptone (20 g L^{-1}), and oleic acid (20 g L^{-1}), buffered with phosphate buffer (100 mM, pH 6.8) were inoculated with cells pregrown in YPD containing of yeast extract (10 g L^{-1}), bactopeptone (10 g L^{-1}), and glucose (10 g L^{-1}) at an initial cell density of $OD_{600} = 0.2$. Stock solutions containing oleic acid (200 g L^{-1}) and Tween40 (5 g L^{-1}) were subjected to sonication three times for 1 min each on ice for emulsification purposes. Cells were incubated at 28 °C for 24 h until complete oleic acid consumption. The cells were removed through centrifugation (10000 rpm for 10 min). Supernatants were directly used in reactions.

Determination of lipase activity: The lipase activity in the culture supernatant was determined by monitoring the hydrolysis of *p*-nitrophenyl butyrate (*p*NPB) into butyrate and *p*-nitrophenol. The method was optimized using 2-methyl-butan-2-ol (2M2B) as solvent to solubilise *p*-nitrophenyl butyrate. Lipase activity was measured in 96-well microplates with Lip2p supernatant (20 μL) containing phosphate buffer (175 μL of a 100 mM solution, pH 7.2), NaCl (100 mM) and of *p*NPB (5 μL of a 40 mM solution) in 2M2B. Activity was measured by following absorbance at 405 nm at 25 °C for 10 min using the VersaMax tunable microplate reader apparatus (Molecular Devices, Rennes, France). One unit of lipase activity was defined as the amount of enzyme releasing 1 μmol of fatty acid per min at 25 °C and pH 7.2

Hydrolysis of 2-bromo phenyl and *o*-tolyl acetic acid esters: Hydrolysis was carried out in Eppendorf tubes (1.5 mL) containing a biphasic medium composed of dried octane (0.3 mL) containing the ester (50 mM) and the aqueous enzymatic solution (0.5 mL). The mixture was shaken in a Vortex Genie 2 (D. Dutscher, Brumat, France). Reactions were realized at 20 °C. At regular time intervals the progress of the reaction was followed by analyzing organic phase composition after phase separation by centrifugation (100 μL diluted in 1 mL hexane).

HPLC analysis: The HPLC device was equipped with a chiral column: Chiralpack OJ (25 cm × 4.6 mm; Daicel Chemical Industries Ltd, Tokyo, Japan) connected to a UV detector (at 254 nm). A flow rate of 1.0 mL min^{-1} was used. The mobile phase was a mixture of *n*-hexane/isopropanol, 80:20 *v/v* for (±)-2-bromo phenyl octyl or ethyl acetate and 98:2 *v/v* for (±)-2-bromo-*o*-tolyl octyl or ethyl acetate.

Determination of enantiomeric excess (*ee*), conversion and enantioselectivity (E): From HPLC results, enantiomeric excess (*ee*) was calculated as defined below [Eq (1)]:

$$ee_s = \{[R]-[S]\}s/\{[R]+[S]\}s \ (s = \text{substrate}) \quad (1)$$

and the conversion [Eq. (2)]:

$$C = 1-\{(R-S)_t/R-S)_{t=0}\} \times 100 \quad (2)$$

The enantioselectivity value was the ratio of initial rate of *R* enantiomer production (vi*R*) versus the initial rate of *S* enantiomer production (vi*S*): $E = (viR/viS)$. The initial rates were determined by linear regression over at least five points before 10% of substrate conversion.

Multiple sequence alignments: Lipase sequence alignments were realized using FUGUE server (http://www-cryst.bioc.cam.ac.uk/~fugue/) (Figure 1). Secondary structure elements were predicted using the software PSIPRED available on the Web (http://bioinf.cs.ucl.ac.uk/psipred), while the secondary structure for templates was taken from the Protein DataBank. The fine adjustment of gap positions was assessed by superimposition of predicted and observed secondary structure.

Model building: A three dimensional model of Lip2p lipase from *Y. lipolytica* was constructed using the program MODELLER implemented in the HOMOLOGY module of the InsightII suite of programs (Accelrys, San Diego, CA, USA) and the sequence alignments obtained above.

The lowest-energy structure predicted using MODELLER was further refined using the CFF91 forcefield implemented within the DISCOVER module of InsightII software suite (Accelrys, San Diego, CA, USA). For the minimization, the CFF91cross terms, a harmonic bond potential, and a dielectric of 1.0 were used. An initial minimization with a restraint on the protein backbone was performed using a steepest descent algorithm followed by conjugated gradient minimization steps until the maximum RMS was less than 0.5. In a subsequent step, the system was fully relaxed. Calculations were performed on a Silicon Graphics O2 workstation.

Acknowledgements

We thank Miguel Angel Cancino for his contribution to the construction of the variant library and we are grateful to David Guieysse for substrate synthesis and for his precious help in the use of the InsightII software

Keywords: bromoarylacetic acid esters · enantioselectivity · enzymes · lipase · mutagenesis · *Yarrowia lipolytica*

[1] S. Erb, *Pharma Technol.* **2006**, Oct. 3.
[2] D. Brady, L. Steenkamp, E. Skein, J. A. Chaplin, S. Reddy, *Enzyme Microb. Technol.* **2004**, *34*, 283–291.
[3] J. Ceynowa, M. Rauchfleisz, *J. Mol. Catal. B* **2003**, *23*, 43–51.
[4] G. S. Choi, J. Y. Kim, J. H. Kim, Y. W. Ryu, G. J. Kim, *Protein Expression Purif.* **2003**, *29*, 85–93.
[5] L. Steenkamp, D. Brady, *Enzyme Microb. Technol.* **2003**, *32*, 472–477.
[6] P. L. A. Overbeeke, J. A. Jongejan, *J. Mol. Catal. B* **2003**, *21*, 89–91.
[7] L. Haughton, J. M. J. Williams, *Synthesis* **2001**, *6*, 943–946.
[8] M. M. Jones, M. J. Williams, *Chem. Commun. (Cambridge, UK)* **1998**, *25*, 19–2520.
[9] S. N. Ahmed, R. J. Kazlauskas, A. H. Morinville, P. Grochulski, J. D. Schrag, M. Cygler, *Biocatalysis* **1994**, *9*, 209–225.
[10] D. Guieysse, C. Salagnad, P. Monsan, M. Remaud-Simeon, *Tetrahedron: Asymmetry* **2003**, *14*, 317–323.
[11] D. Guieysse, C. Salagnad, P. Monsan, M. Remaud-Simeon, *Tetrahedron: Asymmetry* **2003**, *14*, 1807–1817.
[12] D. Guieysse, G. Sandoval, L. Faure, J. M. Nicaud, P. Monsan, A. Marty, *Tetrahedron: Asymmetry* **2004**, *15*, 3539–3543.
[13] M. T. Reetz, M. Puls, J. D. Carballeira, A. Vogel, K. E. Jaeger, T. Eggert, W. Thiel, M. Bocola, N. Otte, *ChemBioChem* **2007**, *8*, 106–112.
[14] R. J. Kazlauskas, *Curr. Opin. Chem. Biol.* **2000**, *4*, 81–88.
[15] K. L. Morley, R. J. Kazlauskas, *Trends Biotechnol.* **2005**, *23*, 231–237.
[16] S. Park, K. L. Morley, G. P. Horsman, M. Holmquist, K. Hult, R. J. Kazlauskas, *Chem. Biol.* **2005**, *12*, 45–54.
[17] S. F. Altschul, T. L. Madden, A. A. Schaffer, J. Zhang, Z. Zhang, W. Miller, D. J. Lipman, *Nucleic Acids Res.* **1997**, *25*, 3389–3402.
[18] J. Pleiss, M. Fischer, M. Peiker, C. Thiele, R. D. Schmid, *J. Mol. Catal. B* **2000**, *10*, 491–508.
[19] R. A. Laskowski, M. W. MacArthur, D. S. Moss, J. M. Thornton, *J. Appl. Crystallogr.* **1993**, *26*, 283–291.
[20] G. Vriend, *J. Mol. Graph.* **1990**, *8*, 52–56.
[21] H. Scheib, J. Pleiss, A. Kovac, F. Paltauf, R. D. Schmid, *Protein Sci.* **1999**, *8*, 215–221.
[22] H. D. Beer, G. Wohlfahrt, J. E. G. McCarthy, D. Schomburg, R. D. Schmid, *Protein Eng.* **1996**, *9*, 507.
[23] R. D. Joerger, M. J. Haas, *Lipids* **1994**, *29*, 377.
[24] M. Cancino, P. Bauchart, G. Sandoval, J.M. Nicaud, I. André, V. Dossat, A. Marty, *Tetrahedron: Asymmetry* **2008**, *19*, 1608–1612.
[25] M. T. Reetz, D. Kahakeaw, R. Lohmer, *ChemBioChem* **2008**, *9*, 1797–1804.
[26] F. Bordes, F. Fudalej, V. Dossat, J. M. Nicaud, A. Marty, *J. Microbiol. Methods* **2007**, *70*, 493–502.
[27] G. Pignede, H. Wang, F. Fudalej, C. Gaillardin, M. Seman, J.-M. Nicaud, *J. Bacteriol.* **2000**, *182*, 2802–2810.

Received: April 7, 2009
Published online on June 5, 2009

